Automated Alignment and On-Sky Performance of the Gemini Planet Imager Coronagraph

Dmitry Savransky[a], Sandrine J. Thomas[b], Lisa A. Poyneer[c], Jennifer Dunn[d], Bruce A. Macintosh[e], Naru Sadakuni[f], Daren Dillon[g] Stephen J. Goodsell[f], Markus Hartung[f], Pascale Hibon[f], Fredrik Rantakyrö[f], Andrew Cardwell[f], Andrew Serio[f] with the GPI team

[a]Sibley School of Mechanical and Aerospace Engineering, Cornell University, Ithaca, NY USA
[b]NASA Ames Research Center, Mountain View, CA USA
[c]Lawrence Livermore National Laboratory, Livermore, CA USA
[d]National Research Council of Canada Herzberg, Victoria, B.C. Canada
[e]Kavli Institute for Particle Astrophysics and Cosmology, Stanford University, Stanford, CA USA
[f]Gemini Observatory, La Serena, Chile
[g]University of California Observatories/Lick Observatory, University of California, Santa Cruz, Santa Cruz, CA USA

Gemini Planet Imager

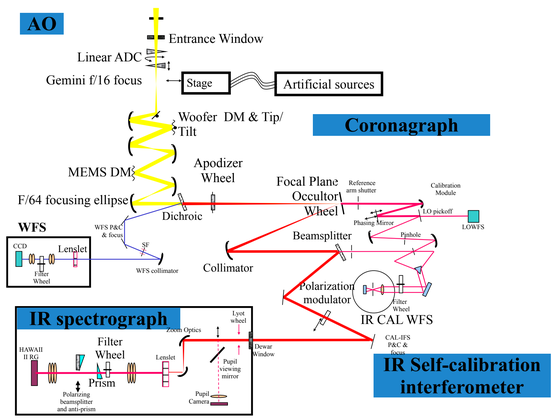

Figure: GPI light path [Macintosh et al., 2008, 2014].

- Adaptive Optics (AO) system - MEMS deformable mirror (DM), piezo-electric DM & Shack-Hartmann wavefront sensor (WFS) correct for atmospheric turbulence and optical errors [See 9148-19]
- Calibration Interferometer (CAL) - IR interferometer reconstructs post-coronagraph wavefront and sends updates to AO [See 9148-224]. Includes low and high order wavefront sensors (LOWFS and HOWFS)
- Integral Field Spectrograph (IFS) - science instrument produces dispersed spectral images [See 9147-55]. Also includes pupil viewing camera immediately behind Lyot plane
- Apodized Pupil Lyot Coronagraph (APLC) for diffraction control composed of Apodizer, Focal Plane Mask (FPM) and Lyot stop [Soummer, 2005]
- GPI Pipeline - Produces reduced 3D data cubes ($x \times y \times \lambda$) in realtime as data is collected [See 9148-224]
- All subsystems are remotely operable and reconfigurable, with multiple open and closed loop controllers constantly running to maintain alignment [See 9147-190 and 9149-87]

Coronagraph components must maintain precise alignment throughout the course of hour-long science observations while GPI moves with the telescope.

Coronagraph Alignment

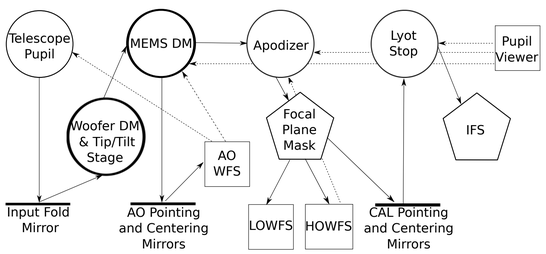

Alignment	Tolerance[a]	Measurement	Achieved[b]
Telescope Pupil to MEMS	0.5%	AO WFS[c] or Pupil viewer	0.012%
AO WFS to MEMS	0.5%	AO WFS	0.019%
Apodizer to MEMS	0.25%	Pupil viewer[d] or HOWFS	0.21%
Lyot Stop to MEMS	1%	Pupil viewer	0.48%

[a]Tolerances are given in percentages of the corresponding pupil size.
[b] RSS errors in tip and tilt on the WFS and errors in x and y on the pupil viewer.
[c] Fractions of sub-apertures, with 43 sub-apertures across the pupil.
[d] The pupil is approximately 232 pupil viewer pixels across.

Figure: Schematic of GPI pupil planes (circles), focal planes (pentagons), wavefront sensors and detectors (squares) and controllable surfaces (thick lines). Solid lines with arrows are the light path, and dashed lines represent imaging of pupil planes. The four pupil planes at the top of the schematic must all be aligned to a common plane—typically the MEMS DM plane [Savransky et al., 2013].

On-Sky Pupil Viewer Coronagraph Images

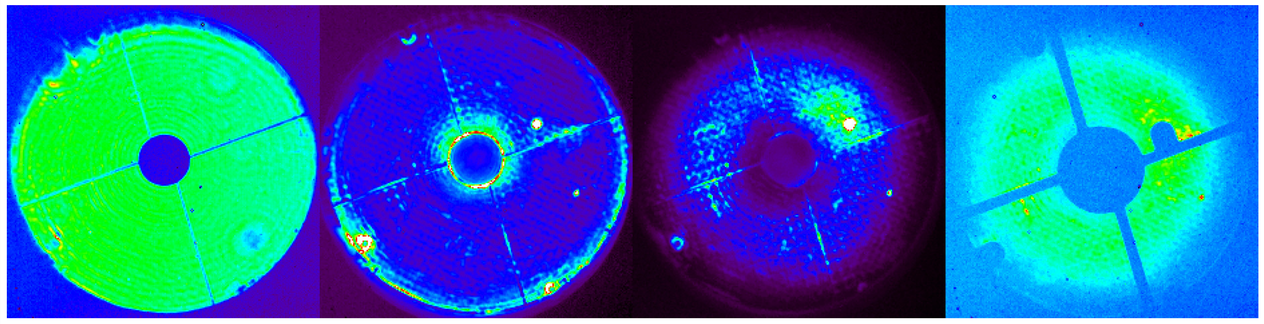

Figure: Pupil viewer images of a 3.2 V magnitude star with all control loops closed and (left to right): 1) No coronagraph—Gemini pupil visible; 2) H band focal plane mask only—the bright spots around the edges of the pupil and in the top-right quadrant are due to bad MEMS DM actuators; 3) FPM and apodizer only; 4) Complete coronagraph. The Lyot stop includes features to block diffracted light from the telescope spiders along with tabs to cover the bad actuators. The regular background pattern is due to features on the MEMS. Each image is individually processed and stretched for visibility—the last image contains less that 10% of the light in the first.

References

B. Macintosh, J. R. Graham, P. Ingraham, Q. Konopacky, C. Marois, M. Perrin, L. Poyneer, et al. First light of the gemini planet imager. *Proceedings of the National Academy of Sciences*, 2014.

B. A. Macintosh, J. R. Graham, D. W. Palmer, R. Doyon, J. Dunn, D. T. Gavel, J. Larkin, B. Oppenheimer, L. Saddlemyer, A. Sivaramakrishnan, et al. The gemini planet imager: from science to design to construction. In *Proc. SPIE*, volume 7015, page 701518, 2008.

D. Savransky, S. J. Thomas, L. A. Poyneer, and B. A. Macintosh. Computer vision applications for coronagraphic optical alignment and image processing. *Applied Optics*, 52(14):3394–3403, 2013.

R. Soummer. Apodized pupil lyot coronagraphs for arbitrary telescope apertures. *The Astrophysical Journal Letters*, 618(2):L161–L164, 2005.

Pupil Alignment

- Pupil plane masks are aligned by imaging them with the IFS pupil viewing camera (with no other coronagraph components in the beam), fitting ellipses to their central obscurations and comparing these fits with a known pattern placed on the MEMS DM
- Corrections are applied in closed loop until these measurements converge

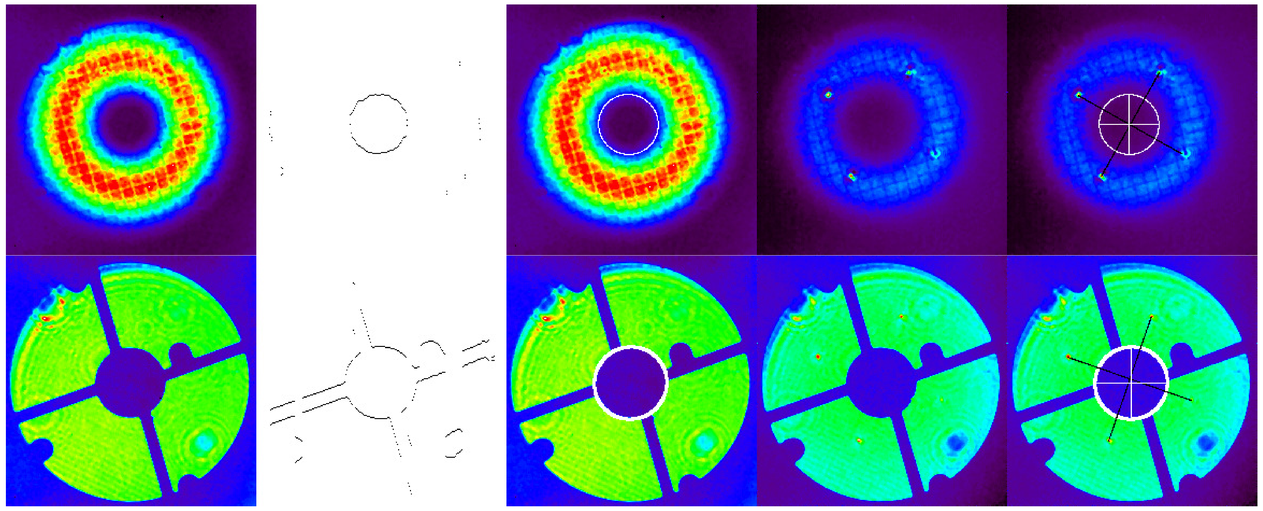

Figure: Alignment of apodizer (top row) and Lyot stop (bottom row) to MEMS DM plane. From left to right: 1) Dark-subtracted, median-filtered pupil viewer image of mask to be aligned. 2) Candidate pixels for ellipse fitting identified by basic edge detection. 3) Best-fit ellipse (white) found via Hough transform. 4) Subtracted pupil viewer images with and without symmetric MEMS DM poke pattern about MEMS center. 5) Line fits to poke pattern (black) and ellipse fit to central obscuration (white) overlaid on original image.

Focal Plane Mask Alignment

- Beam must be actively held centered on FPM pinhole to within 5 mas
- Find initial centering by exploiting symmetry of FPM and maintain using Tip/Tilt measurements from CAL LOWFS

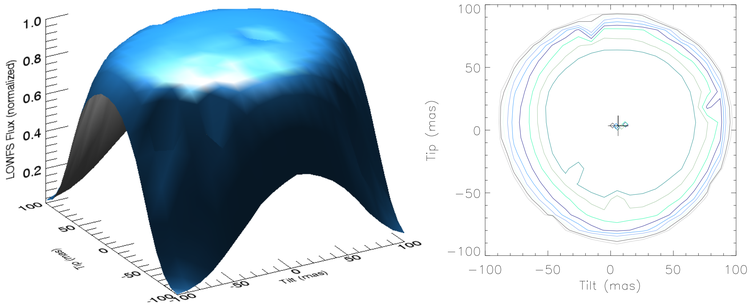

Figure: *Left:* Surface plot of raster scan of the H-band FPM with the LOWFS. *Right:* Least-squares fits to contours of the raster scan, with the centers of each plot marked with diamonds. The cross shows the mean center and error of all of the contours. Pinhole center is found by making symmetric moves over FPM and equalizing measured total LOWFS fluxes.

Figure: (*Below*) Short exposure IFS images and corresponding contrast profiles with *Left:* FPM centered (solid line), *Center:* FPM offset in tip (dashed line), and *Right:* FPM offset in tilt (dash-dotted line). The FPM misalignment causes a contrast degradation near the inner working angle even in single frames, and raises the noise floor on whole observing sequences.

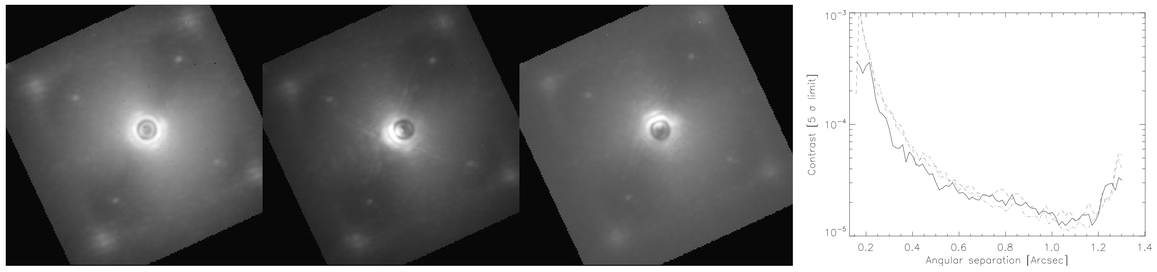

Conclusions and Future Work

- We have developed a robust set of algorithms and procedures for automatically aligning GPI's various coronagraph configurations and maintaining these alignments over observing sequences of one hour or more
- Pupil alignments are good over the course of a whole observing run (one week or more) and can be quickly checked on a daily basis using the same tools
- Our ability to introduce small offsets to various components while in closed loop operation allows us to observe in poor seeing and high wind conditions, outside of GPI's nominal operating range

Acknowledgements: GPI has been supported by Gemini Observatory, which is operated by the Association of Universities for Research in Astronomy, Inc., under a cooperative agreement with the NSF on behalf of the Gemini partnership: the National Science Foundation (United States), the National Research Council (Canada), CONICYT (Chile), the Australian Research Council (Australia), Ministério da Ciência, Tecnologia e Inovação (Brazil), and Ministerio de Ciencia, Tecnología e Innovación Productiva (Argentina). Portions of this work were performed under the auspices of the U.S. Department of Energy by Lawrence Livermore National Laboratory under Contract DE-AC52-07NA27344. The GPI team makes use of Dropbox for sharing large datasets among team members and thanks Dropbox for sponsoring a team account.

 ds264@cornell.edu